Integrated Ferroelectrics, 71: 221–232, 2005

ISSN 1058-4587 print / 1607-8489 online
DOI: 10.1080/10584580590964673

Taylor & Francis
Taylor & Francis Group

Piezoelectric Composites as Bender Actuators

Karla Mossi,[1,*] Robert Bryant,[2] and Poorna Mane[1]

[1]Virginia Commonwealth University, Mechanical Engineering, Richmond, VA 23294, USA
[2]NASA Langley Research Center, MS 226, Hampton, VA 23681, USA

ABSTRACT

Lead Zirconate Titanate, PZT, layered into a composite with different materials, produces pre-stressed, curved, devices capable of enhanced displacement. This study focuses on Thunder and Lipca which are built using different combinations of constituent materials. Thunder devices consist of layers of aluminum, PZT, and stainless steel bonded with a hot-melt adhesive. Lipca devices consist of carbon and fiberglass layers with a PZT layer sandwiched in between them. Measuring out-of-plane displacement under load as a function of temperature is used to evaluate field-dependent stiffness. Results show that Lipca devices have higher stiffness than Thunder at 24°C, but lower at other temperatures.

Keywords: Thunder; Lipca; piezoelectric actuators; piezoelectric devices

INTRODUCTION

Pre-stressed piezoelectric devices are of interest in a variety of aerospace and industrial applications due to their durability and enhanced strain capabilities. This enhanced durability and strain output is due to the combination of piezoelectric ceramics with other materials forming composites. Differences between the thermal and structural properties of the various materials that form the layers of these composites, lead to the pre-stressing of the PZT layer, which creates internal stresses. These stresses combined with restricted lateral motion, are shown to enhance axial displacement.

Some of the parameters that influence the performance of pre-stressed devices are layer configurations, material properties and dimensions, type and thickness of adhesive between layers, clamped or pinned boundary conditions,

Received December 17, 2004; In final form February 8, 2005.
*Corresponding author. E-mail: kmmossi@vcu.edu

and point or distributed loading conditions [1–3]. Design parameters utilized in previous studies of these types of actuators is the thickness ratio of active to inactive layers for several devices [4, 5]. This in turn determines the overall thickness of the composite. Device length and width are dictated by the desired application whether it is for development purposes or research [6]. While many types of pre-stressed actuators exist, Thunder and Lipca are of special interest since these actuators have been investigated numerically and experimentally. However, many factors that affect their performance are still unknown.

Thunder devices manufactured by Face International, Norfolk, VA, are composites made of an active ceramic layer, and one or more inactive metallic layers. The active layer is composed of a piezoelectric ceramic (PZT5A), and the metallic layer is commonly aluminum, stainless steel, or brass [7, 8]. The devices are pre-stressed by processing the composite at 300°C to take advantage of the differences in the coefficients of thermal expansion among the various materials within the actuator. As demonstrated by numerous studies [9–11], these devices have enhanced displacement compared to PZT Unimorphs. The Lipca-C series is manufactured by Konkuk University, Korea [12]. Currently the series is divided into several types, such as C1 and C2. Different layering sequences in the two series lead to differences in the radius of curvature, that could effect displacement capabilities. The layering sequence in Lipca-C2 gives the largest radius of curvature among the devices investigated [13]. Lipca-C2 consists of layers made of glass/epoxy and carbon/epoxy composites with a PZT layer placed between these layers. Both the top and the bottom layers are made of glass/epoxy composite. Below the top layer, there is a layer of carbon/epoxy followed by the PZT layer and finally two layers of glass/epoxy at the bottom. Schematics showing the arrangement of layers in both the devices are shown in Figs. 1a and 1b.

Previous work that compared Lipca and Thunder devices demonstrated that non-loaded Lipca actuators are capable of displacing more than Thunder actuators at the same voltage over a range of frequencies [14]. It is important to note that in the case of Lipca, the electric leads are in direct contact with the piezoelectric ceramic. In the case of the Thunder device, the field applied has to go through the adhesive layer. As a result, the Lipca devices begin to re-pole at lower fields as compared to Thunder. One advantage that Thunder does retain over current Lipca models is their ability to support loads up to 5 N without sustaining permanent damage [15]. To provide more insight on the behavior of these composites, actuator performance as a function of field and temperature loaded and unloaded, as well as other parameters measured from these results are shown.

EXPERIMENTAL SETUP

Experiments were conducted to characterize both free and loaded displacement of pre-stressed piezoelectric actuators over a range of temperatures. The models

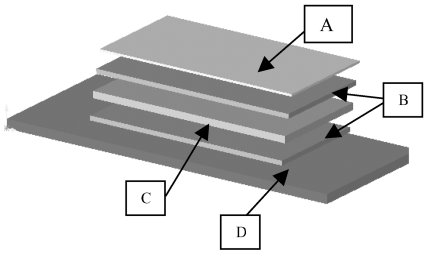

Layer	Material	l	w	t
A	Aluminum	71	24	0.025
B	SI-Film	72.3	24	0.020
C	PZT	72.3	24	0.254
D	Stainless Steel	97	24	0.254

l: length (mm); w: width (mm); t: thickness (mm)

(a)

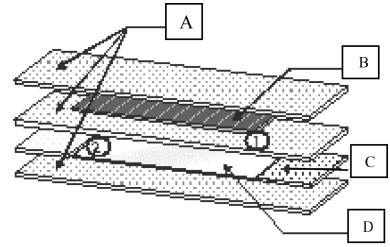

Layer	Material	l	w	t
A	Glass Epoxy	100	24	0.089
B	Carbon Epoxy/Unidirectional	71	22	0.10
C	Glass/Epoxy	14	22	0.10
D	PZT	72.4	23	0.254

l: length (mm); w: width (mm); t: thickness (mm)

(b)

Figure 1. Device and layer compositions (a) Thunder, electrical connections with layers A and D; (b) Lipca-C2, electrical connections with 1 and 2.

tested were, LIPCA-C2 and Thunder. The displacement is measured using a linear voltage displacement transducer, LVDT series 232 Trans Tek Inc, an a National Instruments environmental chamber, Sun Electronics C20, a TREK 10/10B voltage amplifier, and a data acquisition system. A specially designed fixture was constructed to allow for horizontal motion resulting from an applied load of 0 to 5 N. The fixture consists of a fixed support and pinned bearing capable of linear motion in the direction of the applied force as shown in Fig. 2. The bearings used are manufactured by American Linear Manufacturers Inc. model LPA12-1-05. The actuators were tested by applying a sinusoidal input voltage from 100 Volts peak-to-peak to 500 Volts peak-to-peak at a frequency

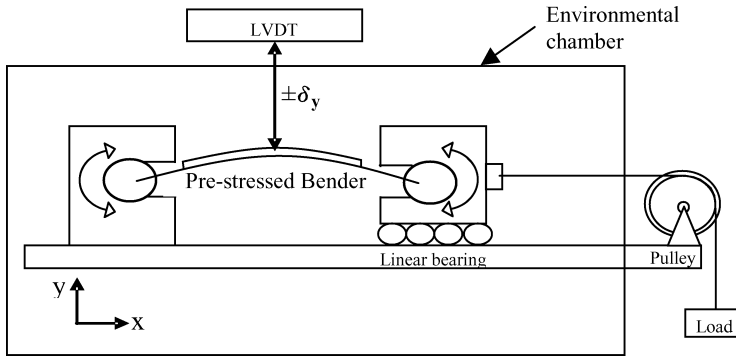

Figure 2. Schemetic of mechanism utilized to load the devices and monitor displacement in an environmental chamber.

of 1 Hz. This was done at quasi-static conditions while varying applied loads between 0 and 5 N. By applying the load to the rotating-sliding mount a uniform distribution of the load throughout the cross-section of the device is achieved at indicated temperatures.

The devices tested are manufactured according to Fig. 1. The PZT, the only common part of these two devices, is approximately the same length, width, and thickness for both types of actuators.

RESULTS AND DISCUSSION

The first set of experiments consisted of measuring the displacement of both actuators while varying the electric field over a range of temperatures with no-load. The temperature range tested was from room temperature to 120°C. Typical results at selected temperatures for an unloaded Thunder device are shown in Fig. 3 with only selected values are included in this figure for clarity purposes. The loops show a large hysteresis and that the temperature effects on the shape of the loops are not pronounced until reaching a temperature of 120°C. At this temperature, with a 0.8 kV/mm peak driving field, 400 Volts peak to peak, the loop starts to show some deformation with the application of negative fields. Another characteristic of the field displacement loops is that the overall hysteresis appears to be smaller at temperatures above ambient.

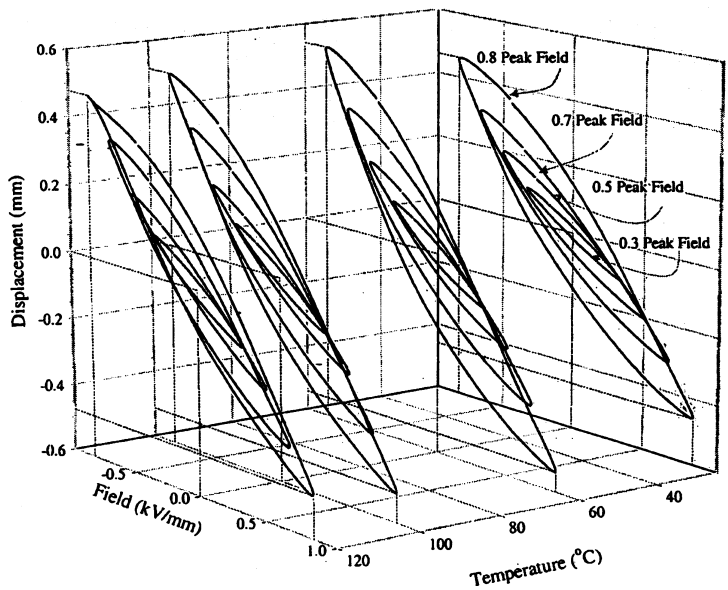

Figure 3. No-load voltage displacement loops for a typical Thunder device.

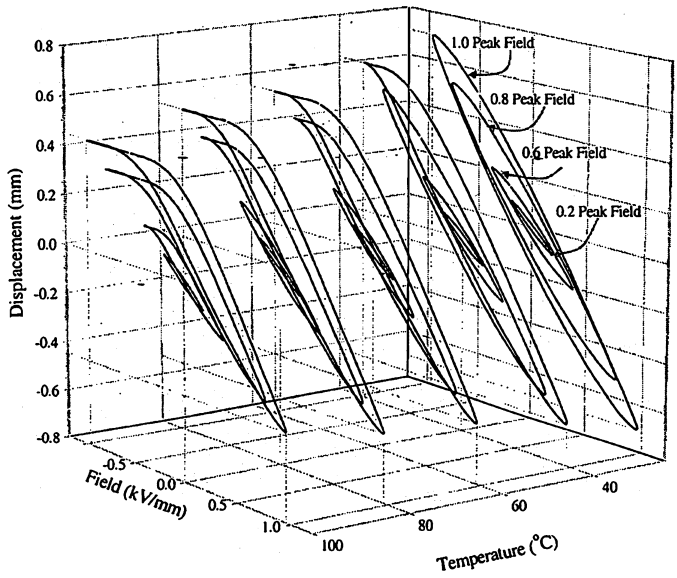

Figure 4. No-load voltage displacement loops for a typical Lipca device.

For a Lipca device, the results for the first set of experiments are shown in Fig. 4. The hysteresis in this case is smaller than Thunder, and the overall displacement at room temperature is higher than Thunder. At 24°C Lipca devices show a 1.5 times higher overall displacement then Thunder devices with smaller hysteresis. Temperature effects are more evident on the Lipca device than the Thunder device at temperatures as low as 40°C at the highest applied field, 1.0 kVp/mm. Loop deformation, defined as the saturation effect, is progressively observed at other temperatures: at 60°C, deformation is evident at 1.0 and 0.8 kVp/mm; at 100°C deformation occurs at 1.0, 0.8, and 0.6 kVp/mm at applied negative fields. Fields lower than 0.6 kVp/mm produced no visible deformations over the temperature range of this experiment.

The second set of experiments involved applying loads at each of the temperatures used in the previous experiment. Figure 5 shows the typical case of de-poling by exceeding the allowable driving field for a Thunder device where load and temperature are applied simultaneously at different magnitudes of driving field. On the loop shown in Fig. 5, possible de-poling of the device is observed at 120°C, with a 5 N applied load. This type of behavior is not observed at any other tested load.

For the Lipca devices, load was not found to have a significant effect on the shape of the loops. For instance, as shown in Fig. 6, at a load of 5 N and the highest applied field, 0.963 kVp/mm the overall displacement does not change significantly with temperature. Loop deformation however, becomes

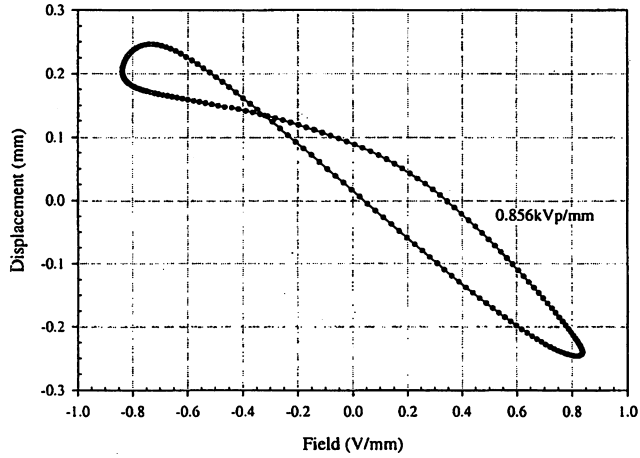

Figure 5. Typical Thunder displacement at 5 N load, 120°C at different peak voltage fields.

apparent at temperatures above 40°C. This loop deformation is evident on Thunder devices at higher temperatures, as shown in Fig. 5. Furthermore, peak to peak displacement at a constant load and varying temperature appears to diminish due to the shape of the loops.

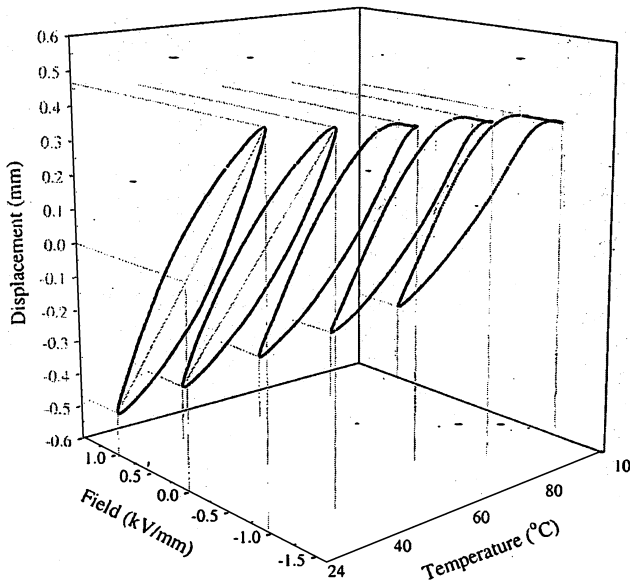

Figure 6. Loaded voltage displacement loop for a Lipca-C2 device at 5 N at different temperatures.

To characterize the displacement of the actuators, an effective field-dependent stiffness in the poling direction, throughout the composite thickness, can be calculated at different operating temperatures. This procedure described in [1] involves calculating the compliance, the inverse of the stiffness, of each actuator. This compliance is calculated for both unloaded and loaded conditions: from a load displacement curve at no field, the mechanical compliance is obtained; from a load displacement curve at different driving fields, compliance that couples mechanical and electrical characteristics at varying fields is obtained. By subtracting these two compliances, an effective field-dependent compliance for the device can be obtained. Stiffness is then calculated as the inverse of this effective field-dependent compliance. In this manner, if mechanical compliance effect is the predominant factor in enhancing the displacement of these composites, then the field-dependent compliance trend for both actuator types should be very similar.

For Thunder devices, peak displacement vs. load follows a linear trend for loads higher than 1 N. This trend, previously documented by Mossi et al. [15] can be observed in Fig. 7. This non-linear trend is attributed to the pre-load effect that this particular type of curved piezoelectric composite exhibits and has been documented by others [10]. This process of calculating the slope of displacement vs. load at different fields can be repeated for all temperatures. By taking a linear fit for all fields at loads higher than 1 N, in order to eliminate the pre-loading effect, a slope can be calculated. It is important to notice also

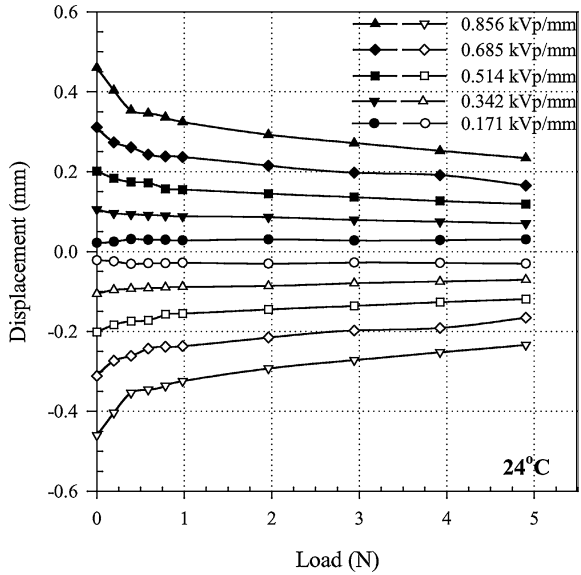

Figure 7. Peak displacement and load at 24°C for a Thunder device.

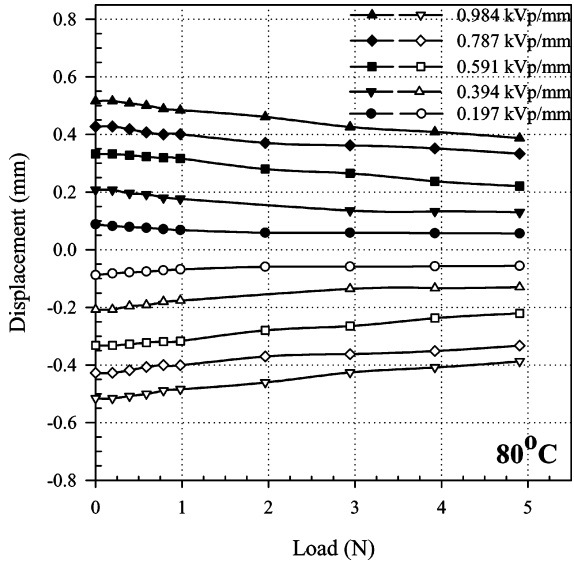

Figure 8. Load vs. displacement peak displacements for a Lipca device at 80°C.

the symmetry of the displacement trends since in some cases asymmetry may be present due to boundary conditions or a DC bias effect. Such asymmetry can be missed if only peak to peak displacement is measured. This asymmetry effect has been observed by others [15], however its causes have not been addressed.

For a Lipca device, the same procedure is followed and a typical set of curves is shown in Fig. 8 at 80°C. The pre-load effect observed on the Thunder devices, is not as pronounced on the Lipca ones, however for consistency purposes loads higher than 1 N are used to calculate stiffness. Note that in this case, as well as for Thunder, there is symmetry on the displacement of the device. Furthermore, displacement remains relatively steady with higher loads. It is important to remember that peak values, may not reflect true maximums when the loops have deformations.

Calculated field-dependent stiffness at different fields and temperatures for both Lipca and Thunder are plotted in Figs. 9 and 10 respectively. For Thunder, field-dependent stiffness increases drastically from room temperature to approximately 40°C. At 40°C and 60°C, the field-dependent stiffness remains constant, and at 80°C stiffness starts to diminish at 120°C. Such behavior indicates that the device field-dependent stiffness depends on temperature, and for a Thunder device, the maximum stiffness values can be obtained at 40°C and 60°C. The field-dependent stiffness for a Thunder device at fields higher than 0.4 kV/mm, varies between 400–800 N/mm. For Lipca devices, a different trend is observed. Field-dependent stiffness decreases steadily with temperature and values range from 400 to 700 N/mm at fields greater than 0.4 kV/mm. These results are shown in Fig. 10.

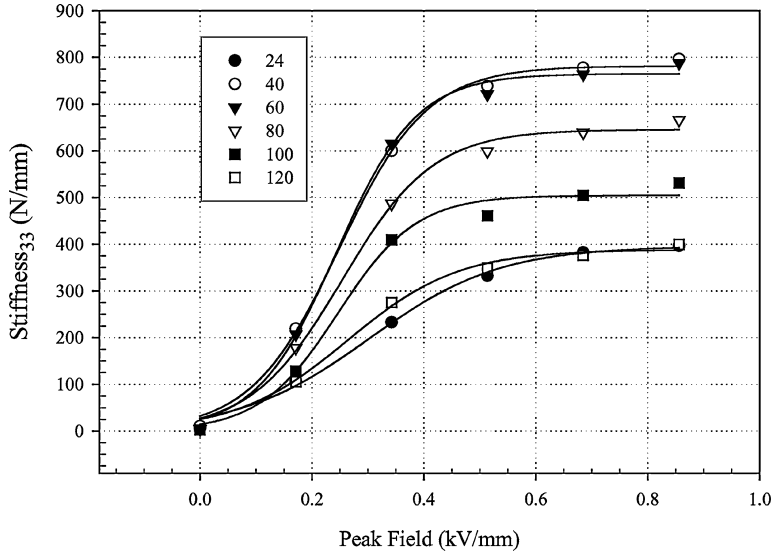

Figure 9. Thunder field-dependent stiffness variations in the direction of the composite thickness when a tension force (0–5 N) is applied in the plane of the composite length, at different temperatures.

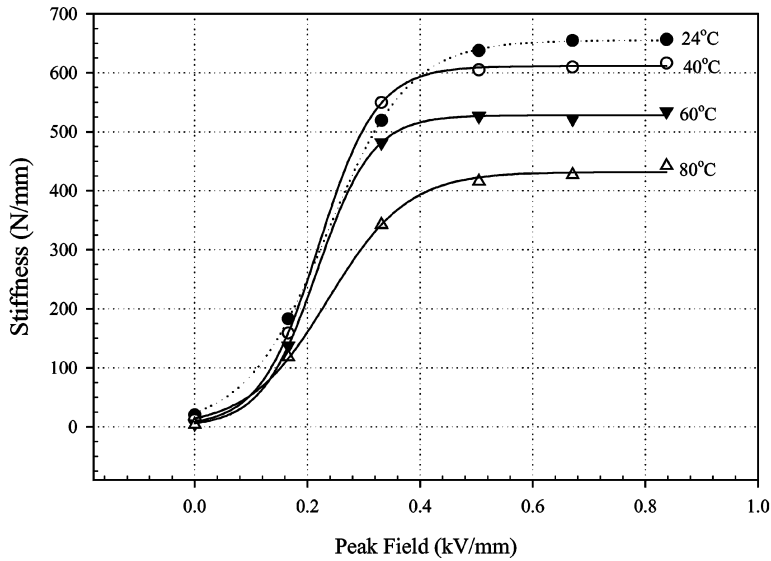

Figure 10. Lipca field-dependent stiffness variations in the direction of the composite thickness when a tension force (0–5 N) is applied in the plane of the composite length, at different temperatures.

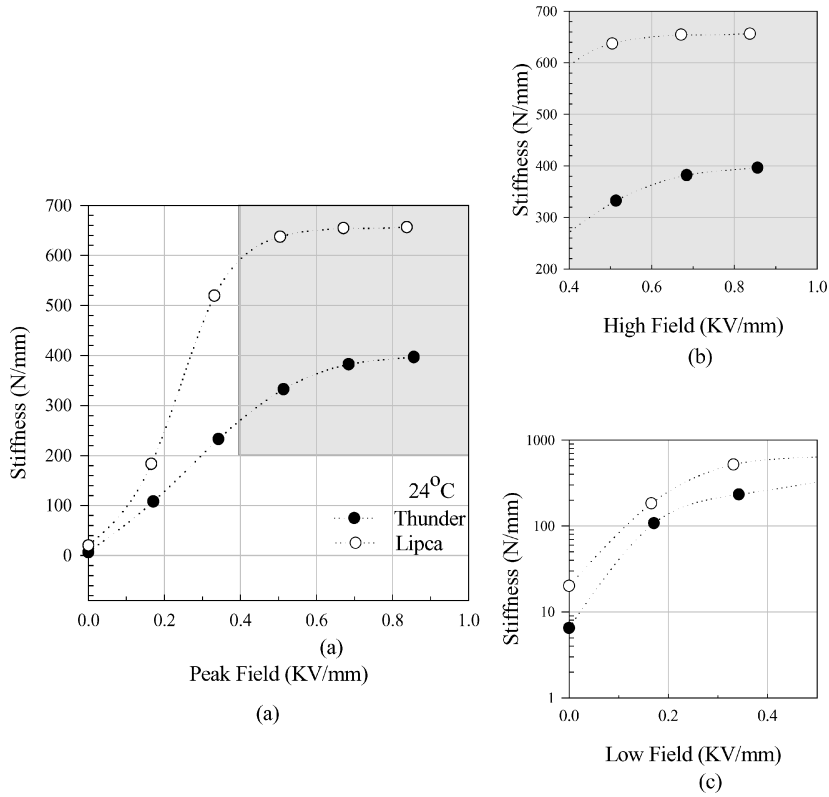

Figure 11. Field-dependent stiffness for Thunder and Lipca at 24°C (a) For the entire applied peak field; (b) For the high peak field ranges; (c) For the low peak field ranges.

Results indicate that the field-dependent stiffness of the Thunder device, shown in Fig. 9, has a peak temperature value not observed in the Lipca devices, Fig. 10. The stiffness for the Lipca devices at higher driving fields, greater than 0.4 kV/mm diminishes with temperature. That is, the peak stiffness for the Lipca device is at room temperature, illustrating that its maximum displacement performance is at room temperature.

To illustrate the different trends obtained for the field-dependent stiffness for Thunder and Lipca, the entire range of applied fields is plotted in Fig. 11a for a temperature of 24°C. The results, illustrated in Figs. 9, 10, and 11a, seem to indicate that at low fields the stiffness is zero. To provide a closer look, Fig. 11b at the high field range, and 11c at the low field range, are shown. At the high fields, the Lipca shows approximately an 85% higher stiffness than Thunder. At the low field range using logarithmic scales, Fig. 11c, it is clear that the values are non-zero and increasing unlike the high field Fig. 11b, where the values of stiffness reach a steady range of values.

The presented results indicate that if mechanical compliance effect is the predominant factor in enhancing the displacement of these composites, then the field-dependent compliance trend for both actuator types may show some similarities. Results shown in Figs. 9, 10, and 11 suggest the possibility of piezoelectric properties being significantly enhanced by other mechanical properties not taken into account. Hence mechanical properties of the composite may play a mayor role on the performance of these actuators.

CONCLUSIONS

The displacement of two pre-stressed actuators, LIPCA and Thunder, are studied at varying loads and temperatures. Previous work shows that the Lipca devices are not just lighter, but their displacement performance is higher than that of the Thunder devices under no-load conditions. Devices utilized were manufactured with PZT of approximately the same width, length, and thickness though the layer distribution is different and the materials utilized are also different. The maximum peak to peak displacement of a Thunder device is approximately 1.0 mm (29% less than Lipca, 1.4 mm) at room temperature. Lipca exhibits large loop deformations at lower temperatures and loads than Thunder. For instance, Lipca exhibits deformations at 40°C with L = 0 N, and at 60°C with L = 3 N. Thunder exhibits deformations at 120°C with L = 0 N and L = 3 N. A Lipca device exhibits at 24°C a field-dependent stiffness higher than a Thunder device. At all other temperatures, thunder has a higher field-dependent stiffness. Field-dependent stiffness of Lipca devices decreases with temperature at fields above 0.4 kV/mm. For the Thunder devices, stiffness varies with temperature, reaching a maximum value at 40°C. The dissimilarities on the field-dependent stiffness suggest the possibility of piezoelectric properties being enhanced significantly by other mechanical properties not taken into account and might play a significant role on the overall performance of these actuators.

The difference in the stiffness of Thunder vs. Lipca at different temperatures may be due to the fact that Lipca is not the result of thermal processing, but of a mechanical pre-stress that occurs with bending the laminate over a curve and curing the epoxy at room temperature.

ACKNOWLEDGMENTS

This work is supported by NASA Langley Research Center grant NNL04AA04G. In addition the authors would like to thank the technical contributions of Greg Graf, Kyle Howerton, Justin Maddox, and Byron Smith.

REFERENCES

1. J. Mulling, T. Usher, B. Dessent, J. Palmer, P. Franzon, E. Grant, and A. Kingon, *Sens. and Actuators A: Phys.* **94**, 19 (2001).
2. K. Mossi, R. Bishop, R. Smith, and H. Banks, *Proc. SPIE Int. Soc. Opt. Eng*. **3667**, 783 (1999).
3. R. Schwartz and M. Narayanan, *Sens. and Actuators A: Phys.* **101**(3), 322 (2002).
4. Z. Ounaies, K. Mossi, R. Smith, and J. Berndt, *Proc. SPIE Int. Soc. Opt. Eng*. **4333**, 399 (2001).
5. S. A. Wise, *Sens. and Actuators A: Phys.* **69**, 33 (1998).
6. N. Lobontiu, M. Goldfarb, and E. Garcia, *Mech. Mach. Theory* **36**, 425 (2001).
7. K. Mossi and R. Bishop, *Proc. SPIE Int. Soc. Opt. Eng*. **3675**, 43 (1999).
8. K. Mossi, G. Selby, and R. Bryant, *Mater. Lett*. **35**, 39 (1998).
9. B. K. Taleghani and J. F. Campbell, *Proc. SPIE Int. Soc. Opt. Eng.* **3668**, 555 (1999).
10. R. Schwartz and M. Narayanan, *Sens. and Actuators A: Phys*. **101**, 322 (2002).
11. R. Wieman, R. Smith, Z. Ounaies, and J. Bernd, *Proc. SPIE Int. Soc. Opt. Eng*. **4326**, 252 (2001).
12. J. Yoon, S. Shin, H. Park, and N. Goo, *Smart Mater. Struct*. **11**, 163 (2002).
13. K. Park, Y. Kim, H. Park, and K. Yoon, *Proc. SPIE Int. Soc. Opt. Eng.* **4699**, 315 (2002).
14. K. Mossi, Z. Ounaies, R. Smith, and B. Ball, *Proc. SPIE Int. Soc. Opt. Eng.* **5053**, 423 (2003).
15. K. Mossi, J. Costley, Z. Ounaies, and R. Bryant, *Proc. SPIE Int. Soc. Opt. Eng.* **5387**, 432 (2004).